



A Simple SERS-Based Trace Sensing Platform Enabled by AuNPs-Analyte/AuNPs Double-Decker Structure on Wax-Coated Hydrophobic Surface

Huixiang Wu^{1,2}, Yi Luo³, Yikun Huang⁴, Qiuchen Dong⁴, Changjun Hou¹, Danqun Huo^{1*}, Jing Zhao³ and Yu Lei^{2,4*}

¹ Key Laboratory for Biorheological Science and Technology of Ministry of Education, State and Local Joint Engineering Laboratory for Vascular Implants, Bioengineering College of Chongqing University, Chongqing, China, ² Department of Chemical and Biomolecular Engineering, University of Connecticut, Storrs, CT, United States, ³ Department of Chemistry, University of Connecticut, Storrs, CT, United States, ⁴ Department of Biomedical Engineering, University of Connecticut, Storrs, CT, United States

OPEN ACCESS

Edited by:

Huan-Tsung Chang,
National Taiwan University, Taiwan

Reviewed by:

Yang-Wei Lin,
National Changhua University of
Education, Taiwan
Lingxin Chen,
Yantai Institute of Coastal Zone
Research (CAS), China

*Correspondence:

Danqun Huo
huodq@cqu.edu.cn
Yu Lei
yu.lei@uconn.edu

Specialty section:

This article was submitted to
Analytical Chemistry,
a section of the journal
Frontiers in Chemistry

Received: 23 August 2018

Accepted: 21 September 2018

Published: 16 October 2018

Citation:

Wu H, Luo Y, Huang Y, Dong Q,
Hou C, Huo D, Zhao J and Lei Y
(2018) A Simple SERS-Based Trace
Sensing Platform Enabled by
AuNPs-Analyte/AuNPs
Double-Decker Structure on
Wax-Coated Hydrophobic Surface.
Front. Chem. 6:482.
doi: 10.3389/fchem.2018.00482

In this work, a simple and versatile SERS sensing platform enabled by AuNPs-analyte/AuNPs double-decker structure on wax-coated hydrophobic surface was developed using a portable Raman spectrometer. Wax-coated silicon wafer served as a hydrophobic surface to induce both aggregation and concentration of aqueous phase AuNPs mixed with analyte of interest. After drying, another layer of AuNPs was drop-cast onto the layer of AuNPs-analyte on the substrate to form double-decker structure, thus introducing more “hot spots” to further enhance the Raman signal. To validate the sensing platform, methyl parathion (pesticide), and melamine (a nitrogen-enrich compound illegally added to food products to increase their apparent protein content) were employed as two model compounds for trace sensing demonstration. The as-fabricated sensor showed high reproducibility and sensitivity toward both methyl parathion and melamine detection with the limit of detection at the nanomolar and sub-nanomolar concentration level, respectively. In addition, remarkable recoveries for methyl parathion spiked into lake water samples were obtained, while reasonably good recoveries for melamine spiked into milk samples were achieved. These results demonstrate that the as-developed SERS sensing platform holds great promise in detecting trace amount of hazardous chemicals for food safety and environment protection.

Keywords: wax, gold nanoparticles, surface enhanced Raman scattering, methyl parathion, melamine

INTRODUCTION

Surface enhanced Raman scattering (SERS) has been drawing increasing attention in the field of analytical chemistry and life science since its first introduction about 40 years ago (Fleischmann et al., 1974; Albrecht and Creighton, 1977; Jeanmaire and Dwyne, 1977; Freeman et al., 1995; Wang et al., 2013; Zhou et al., 2016). SERS enhancement derives from giant electromagnetic

field enhancement enabled by localized surface plasmon resonance (LSPR) “hot spots,” which are typically formed at small gaps (usually <10 nm) between noble metal nanoparticles, with an enhancement factor up to 10^{12} (Kleinman et al., 2013). Compared with traditional bulky instruments, for instance gas chromatography (Vesely et al., 2003), liquid chromatography (Hogard et al., 2017), high-performance liquid chromatography (Özyürek et al., 2012) etc., SERS based detection can be realized using a portable Raman spectrometer, which displays several advantages, such as portability, easy accessibility, cost effectiveness, and rapid analysis. These advantages endow its potential use in point-of-care and in-field trace sensing applications.

Gold nanoparticles (AuNPs) have been widely employed as SERS substrates because they offer very strong Raman enhancing effect (Lou et al., 2011; Li J. J. et al., 2015; Jiang et al., 2017). Furthermore, excellent size and shape tunability of AuNPs make it possible to optimize the enhancement factor for desired SERS detection. To date, scores of reports have been published on AuNPs-based SERS for the detection and discrimination of DNA (Lim et al., 2010), anticancer drugs (Ilkhani et al., 2016; Kurzatkowska et al., 2017), amino acid (Schwartzberg et al., 2004), melamine (Lee et al., 2007; He et al., 2011; Kim et al., 2012; Giovannozzi et al., 2014; Rajapandiyam et al., 2015), biothiols (Liu et al., 2017), various pesticides (Nguyen et al., 2014; Alsammarrarie and Lin, 2017; Cao et al., 2017; Fortuni et al., 2017; Jiang et al., 2017; Tan et al., 2017), and other hazardous chemicals (Li et al., 2011). For example, Giovannozzi et al. (2014) presented a simple AuNPs based SERS system in aqueous solution for melamine detection, in which colloidal AuNPs displayed satisfactory SERS enhancement with a limit of detection of $1.35 \mu\text{M}$ melamine. Although acceptable sensitivity and reproducibility have been obtained for melamine detection in aqueous solution, more sensitive detection for hazardous chemicals is still highly demanded, especially for the detection of highly toxic compounds such as pesticides.

Generally, SERS detection of analyte on solid state substrates is much more sensitive than detection of analyte in aqueous solutions due to the formation of more “hot spots” among adjacent nanoparticles. A host of SERS substrates were fabricated based on highly homogeneous noble metal nanostructures (e.g., Au nanorod arrays) to improve the reproducibility (Kim et al., 2012; Peng et al., 2013; Wallace et al., 2014; Yu et al., 2015; Wang et al., 2016). Although favorable repeatability and excellent sensitivity toward targets can be achieved by using those SERS substrates, relatively high-cost associated with complicated fabricating processes could potentially hinder their wide applications. Alternatively, the use of hydrophobic substrate can also enhance sensitivity and reproducibility of the SERS based sensor system. In this scheme, small volume of aqueous samples were dropped on a hydrophobic substrate and allowed to evaporate. The evaporation process created a higher number of “hot spots” in confined area and better uniformity of nanomaterials distribution. Accordingly, many efforts have been made to produce and employ hydrophobic SERS substrates for enhanced SERS sensing (Li et al., 2014; Wallace et al.,

2014; Cheung et al., 2016; Jayram et al., 2016). However, a simple method to fabricate hydrophobic substrate is still highly demanded.

In this work, we present a simple and versatile SERS sensing platform enabled by AuNPs-analyte/AuNPs double-decker structure on wax-coated hydrophobic surface using a portable Raman spectrometer. The simplicity, cost-effectiveness, and easiness to handle in coating are three greatest merits of wax serving as a hydrophobic material, compared to other hydrophobic materials in SERS applications. Wax-coated silicon wafer served as a hydrophobic surface to induce both aggregation and concentration of AuNPs mixed with analyte of interest. After drying, another layer AuNPs of aqueous phase was drop-cast onto the layer of AuNPs-analyte on the substrate to form a double-decker structure, inducing more “hot spots” to further enhance the Raman signal. Specifically, AuNPs with diameters of 60 and 130 nm were employed for SERS detection of two model compounds, methyl parathion and melamine (chemical structure shown in **Figure 1**) respectively, to demonstrate the feasibility of the developed SERS sensing platform for environment and food safety monitoring. The SERS sensor showed high sensitivity with a detection limit at nanomolar/sub-nanomolar level toward the two target molecules, with satisfactory reproducibility. In addition, the sensor was able to detect both methyl parathion spiked into lake water with remarkable recovery and melamine spiked into milk with reasonably good recovery. These results suggest that this simple, low cost, and versatile SERS sensing platform can offer a promising strategy for ultrasensitive detection of hazardous chemicals in real samples.

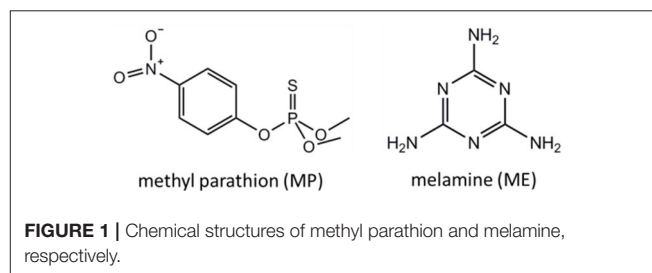
MATERIALS AND METHODS

Chemicals and Reagents

Chloroauric acid ($\text{HAuCl}_4 \cdot 4\text{H}_2\text{O}$, $\geq 99.9\%$ trace metals basis), hydroxylamine hydrochloride ($\text{NH}_2\text{OH} \cdot \text{HCl}$), methyl parathion ($\text{C}_8\text{H}_{10}\text{NO}_5\text{PS}$, denoted as MP) and melamine ($\text{C}_3\text{H}_6\text{N}_6$, denoted as Me) were acquired from Sigma-Aldrich. Sodium citrate ($\text{Na}_3\text{C}_6\text{H}_5\text{O}_7 \cdot 2\text{H}_2\text{O}$) was purchased from Fisher Scientific. All of the chemicals were used without any purification.

Instrument and Apparatus

UV-vis spectra of colloidal AuNPs were recorded on a UV-spectrometer (Cary 60, Agilent Technologies). Transmission electron microscopy (TEM) images and scanning electron



microscopy (SEM) images were acquired using FEI Tecnai G2 Spirit BioTWIN and FEI Nova NanoSEM 450, respectively. A portable Raman spectrometer (QE Pro, Ocean Optics), coupled with a 785 nm laser (operated at 35 mW), was used to collect the Raman spectra. For each Raman measurement, the spectrum was integrated for 5 s.

Preparation of AuNPs

Sixty nanometers of AuNPs were prepared using Frens' method (Frens, 1973). Briefly, 1.06 mg of chloroauric acid aqueous solution (0.0254 M) was added into a 250 mL round-bottomed flask loaded with 99 mL distilled water and heated to boil. After that, 1.0 mL of freshly prepared sodium citrate aqueous solution (0.0388 M) was added into the mixture with stirring and kept boiling for another 20 min. Finally, 60 nm AuNPs were obtained after turning off the heating and cooling to room temperature with stirring.

A seed mediated method was used to synthesize 130 nm AuNPs according to previous report (Tian et al., 2013). In detail, 4 mL of as-prepared 60 nm AuNPs, 900 μ L of freshly prepared sodium citrate aqueous solution (0.0388 M) and 52 mL deionized water were successively loaded into the flask with stirring for 5 min. To the above solution, 0.88 mL of aqueous chloroauric acid solution (0.0254 M) was quickly added and kept stirring for another 5 min. After that, 700 μ L of freshly prepared hydroxylamine hydrochloride aqueous solution (0.0101 M) was injected into above mixture solution twice and the reaction solution was incubated for 2 h to yield AuNPs with an average diameter of about 130 nm.

Preparation of Methyl Parathion and Melamine Samples

Methyl parathion stock solution (0.01 M) was prepared by adding 0.0263 g of methyl parathion into 10 mL absolute ethanol, while melamine stock solution (0.01 M) was prepared by adding 0.0126 g of melamine into 10 mL of deionized water. Methyl parathion ethanol solutions and melamine aqueous solutions with certain concentrations were obtained by diluting the stock solutions using ethanol and deionized water correspondingly.

Preparation of Spiked Real Samples

Lake water sample was collected from Swan Lake at the University of Connecticut and filtered through an ordinary filter paper to remove any large solid particles. Methyl parathion spiked lake water samples were then prepared by quantitatively adding appropriate amount of methyl parathion stock solution into lake water samples and finally subject to SERS detection in recovery studies.

Milk samples (purchased from a local grocery store) were first spiked with certain concentrations of melamine and then pretreated according to a previous report with some modifications for recovery studies (Hu et al., 2015). Briefly, milk samples (0.5 mL) spiked with different concentration of melamine were added into 4.5 mL methanol and shaken for 1 min, followed by sonication for 10 min. And then, the mixtures were centrifuged for 10 min at 12,000 rpm. Supernatants were collected and subject to SERS detection in recovery studies.

SERS Measurement Procedure

The typical SERS sensing procedure developed in this study is presented in **Figure 2** and briefly described below. Commercial wax was first heated and melted into liquid state in a crucible. Then liquid wax was poured onto a silicon wafer, immediately followed by spreading using a glass rod before its solidification, thus generating a thin layer of wax to offer an excellent hydrophobic surface. Next, 5 μ L methyl parathion samples or melamine samples were added into 45 μ L AuNPs (with certain particle size) aqueous solutions and incubated for 5 min to form AuNPs-analyte mixture solution. Next, 5 μ L AuNPs-analyte mixture solution were dropped onto the wax-coated surface and left to dry in ambient conditions. After drying, 5 μ L of AuNPs solution were subsequently dropped onto the dried spot and allowed to dry again. Finally, Raman scattering spectra were recorded from the dried spots using a portable Raman spectrometer.

RESULTS AND DISCUSSION

Characterization of AuNPs

UV-vis spectroscopy and TEM were employed to determine the absorption spectrum and morphology of the AuNPs. As shown in **Figure 3A**, UV-vis spectrum of the as-prepared 60 nm AuNPs suspension has a narrow peak at 538 nm, indicating that AuNPs were monodispersed. To further examine the morphology of the 60 nm AuNPs, TEM image was collected. From **Figure 3C** and its inset, one can see that the AuNPs show good size-uniformity with an average diameter of about 60 nm. Similarly, **Figure 3B** shows the UV-vis spectrum of the as-prepared 130 nm AuNPs synthesized. A relatively broad peak was observed with a peak wavelength of 593 nm, suggesting lower size uniformity than that of the 60 nm AuNPs. From the TEM image in **Figure 3D**, the AuNPs have an average diameter of about 130 nm, with some variation in their shapes, such as sphere, polyhedron and rod-like. The concentration of the as-prepared 60 and 130 nm AuNPs was calculated to be 0.0250 and 0.0058 nM, respectively, according to its UV-vis spectrum and a reported method (Haiss et al., 2007). And the as-prepared 60 and 130 nm AuNPs were then utilized for subsequent SERS studies.

Hydrophobicity of Wax-Coated Silicon Wafer

In this study, hydrophobicity of the substrate plays important roles in both the reproducibility and the sensitivity of SERS sensor. **Figures 4A,B** show the photograph of a 5 μ L water droplet on the silicon wafer and a thin layer of wax-coated silicon wafer, respectively. The diameter (ca. 2 mm) of the water droplet on the wax-coated silicon wafer was obviously smaller than that (ca. 3 mm) on the bare silicon wafer, suggesting good hydrophobicity of the simple wax coating. To further study the hydrophobicity of wax-coated silicon wafer, the liquid-solid contact angle test was carried out. As shown in **Figure 4C**, a contact angle of 61.9° was observed for water droplet on bare silicon wafer. In comparison, the contact angle for wax-coated silicon wafer was measured to be 112.3° according to **Figure 4D**, confirming the much higher hydrophobicity of wax-coated

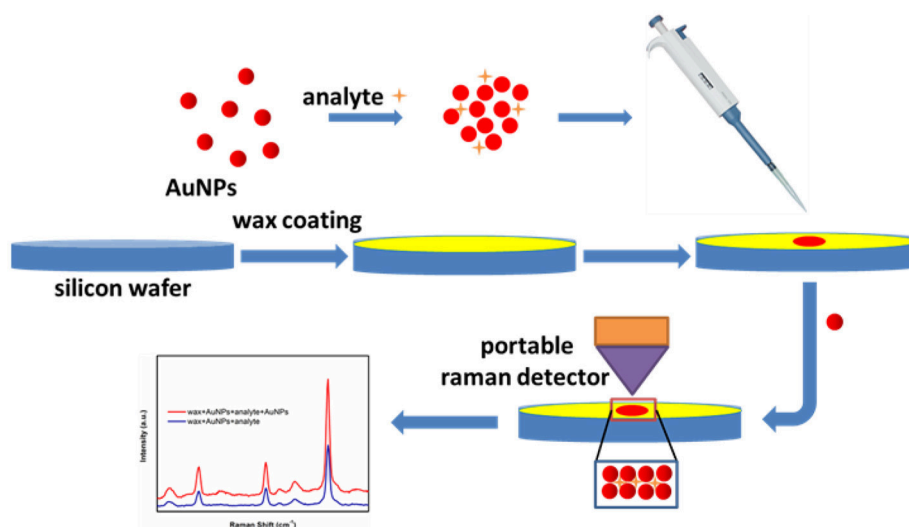


FIGURE 2 | Schematic of the SERS-based trace sensing platform enabled by AuNPs-analyte/AuNPs double-decker structure on wax-coated hydrophobic surface.

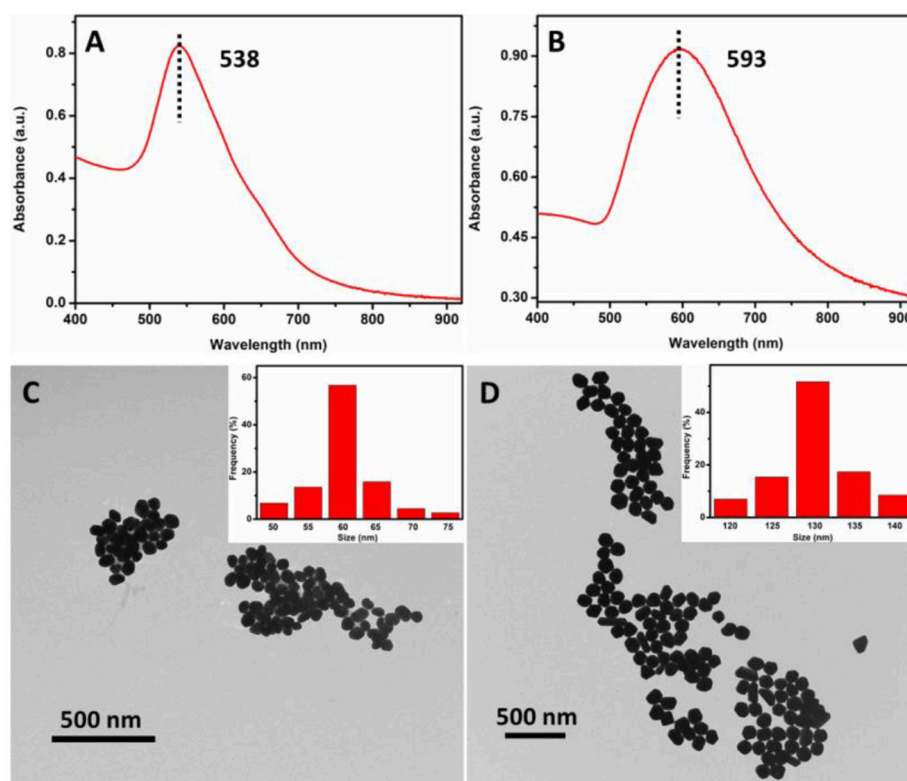


FIGURE 3 | UV-vis spectra (A,C) and TEM images (B,D) of the as-prepared 60 and 130 nm AuNPs, respectively.

silicon wafer than the bare one. To examine the morphology of the AuNPs layer on the substrate, 60 nm AuNPs were first added on the wax-coated silicon wafer. Due to the hydrophobicity of the substrate, the AuNPs typically formed small aggregates on the substrate (data not shown). After the addition of another

layer of AuNPs, a dense AuNPs aggregates formed as seen from **Figure 4E**. One can see that a great number of gaps formed in the AuNPs aggregates, which serve as “hot spots” for SERS detection. Similar phenomena were observed for 130 nm AuNPs on substrates (**Figure 4F**). The data suggest that the wax coating

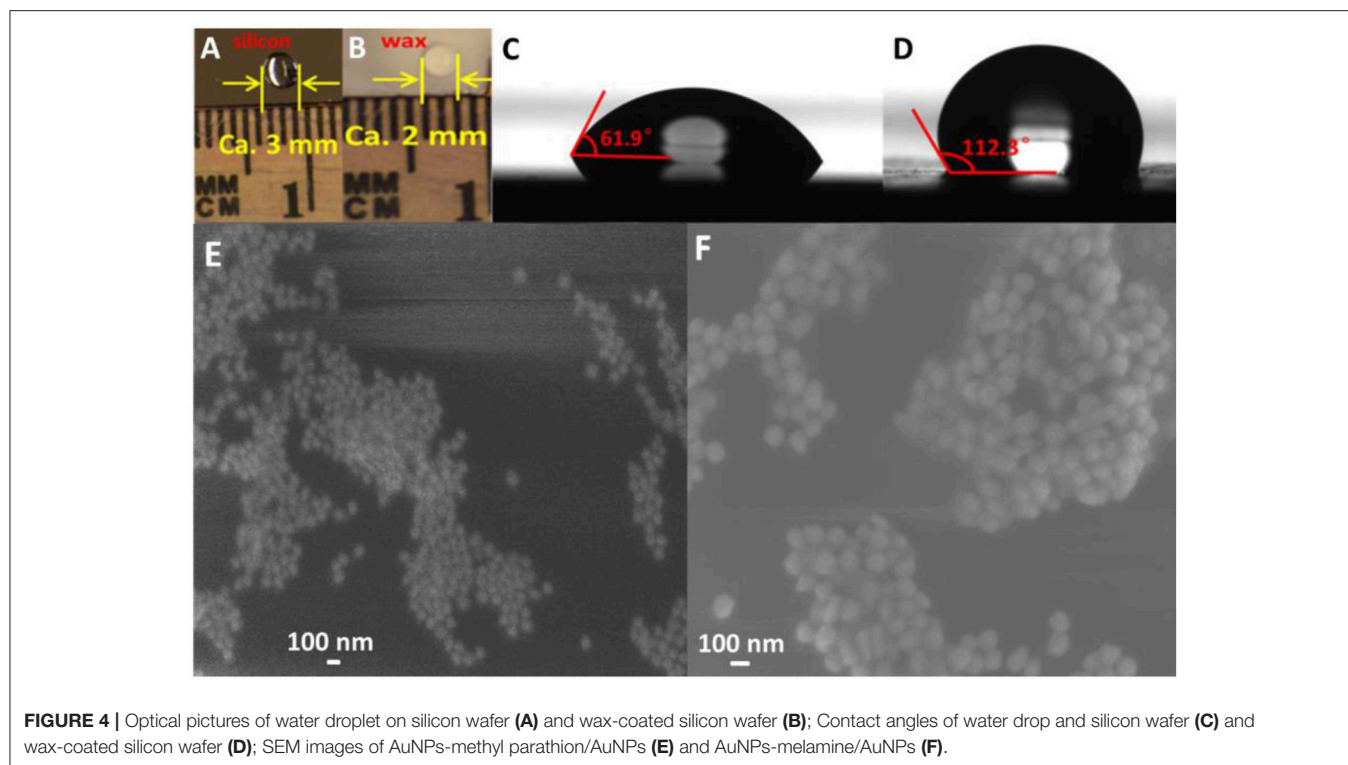


FIGURE 4 | Optical pictures of water droplet on silicon wafer (A) and wax-coated silicon wafer (B); Contact angles of water drop and silicon wafer (C) and wax-coated silicon wafer (D); SEM images of AuNPs-methyl parathion/AuNPs (E) and AuNPs-melamine/AuNPs (F).

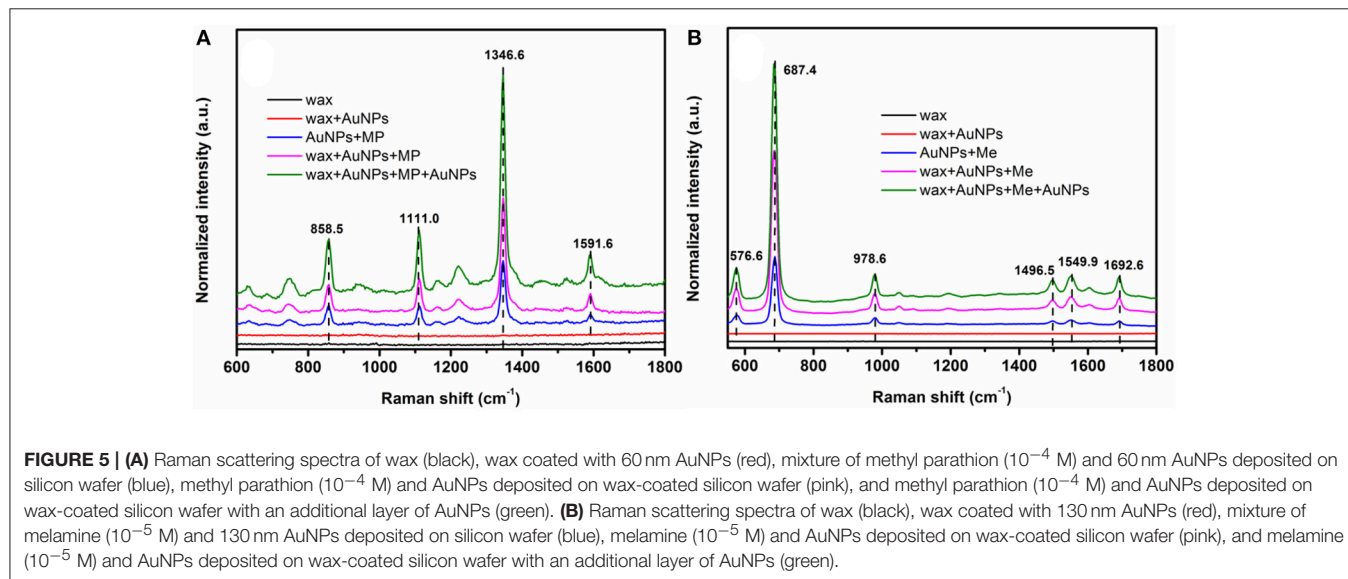


FIGURE 5 | (A) Raman scattering spectra of wax (black), wax coated with 60 nm AuNPs (red), mixture of methyl parathion (10^{-4} M) and 60 nm AuNPs deposited on silicon wafer (blue), methyl parathion (10^{-4} M) and AuNPs deposited on wax-coated silicon wafer (pink), and methyl parathion (10^{-4} M) and AuNPs deposited on wax-coated silicon wafer with an additional layer of AuNPs (green). (B) Raman scattering spectra of wax (black), wax coated with 130 nm AuNPs (red), mixture of melamine (10^{-5} M) and 130 nm AuNPs deposited on silicon wafer (blue), melamine (10^{-5} M) and AuNPs deposited on wax-coated silicon wafer (pink), and melamine (10^{-5} M) and AuNPs deposited on wax-coated silicon wafer with an additional layer of AuNPs (green).

on silicon wafer induced aggregation of the AuNPs, and the additional layer of AuNPs introduced more “hot spots,” thus enhancing the sensitivity in subsequent SERS measurement.

Raman Spectra Intensities of Targets Performed on Various Substrates

Better hydrophobicity of the substrate, on one hand, can shrink the AuNPs-analyte droplet during evaporation and lead to higher target concentration and more “hot spots” in the probe spot, enhancing the sensitivity. On the other hand, better

hydrophobicity of the substrate improves the uniformity of the distribution of AuNP-analyte complexes on the substrate after drying, thus favoring better reproducibility of SERS sensing. As shown in Figure 5, Raman scattering peak intensities of the analyte on wax-coated silicon wafer were much stronger than that on the bare silicon wafer, for both of methyl parathion and melamine, at the same analyte concentration. In addition, no obvious Raman scattering peak was observed for wax with or without AuNPs coating (black and red lines in Figures 5A,B), indicating that wax did not interfere with

the Raman measurement. Four strong peaks appeared at 858.5 cm^{-1} , 1111.0, 1346.6, and 1591.6 cm^{-1} in the Raman spectra collected from methyl parathion on 60 nm AuNPs on silicon wafer (blue line in **Figure 5A**). They can be assigned to the stretching vibration of P-O and C-N, bending vibration of C-H and phenyl stretching, respectively, in accordance with previous report (Li Z. et al., 2015). Peaks at identical positions with stronger intensities were observed in the Raman spectra for AuNPs-methyl parathion on wax-coated silicon wafer (pink line in **Figure 5A**). Similar phenomena were observed in **Figure 5B** for complex of AuNPs (130 nm) and melamine on silicon wafer. Specifically for melamine detection, the strongest Raman peak at 687.4 cm^{-1} was attributed to ring breathing. Peaks at 576.6, 978.6, 1496.5, 1549.9, and 1692.6 cm^{-1} were comprehensively ascribed to vibrations of C-N and N-H (Mircescu et al., 2012). All these distinct assignments were listed in **Table 1**. Clearly, intensities of these peaks of AuNPs-melamine on wax-coated

silicon wafer were much stronger than those on bare silicon wafer.

“Hot spots” have been demonstrated to be extremely important for SERS based sensing (Camden et al., 2008; Kubackova et al., 2015; Zhang et al., 2017). In order to further improve the sensitivity of the sensor, another AuNPs layer was coated onto the AuNPs-analytes on wax, forming a spot of AuNPs-analytes/AuNPs double-decker structure on wax. The additional AuNPs coating can substantially increase the amount of small gaps between AuNPs-analytes and AuNPs, resulting in a sandwich-like AuNP/analyte/AuNP structure. As a result, intensities of the Raman scattering peaks of wax/AuNPs-methyl parathion/AuNPs were significantly increased compared to that of wax/AuNPs-methyl parathion (green line in **Figure 5A**). Similar observation was made for melamine as shown in **Figure 5B**. The results demonstrate that the wax/AuNPs-analytes/AuNPs detection strategy developed here can potentially detect methyl parathion and melamine with high sensitivity.

TABLE 1 | Raman scattering peaks assignment for methyl parathion and melamine (Mircescu et al., 2012; Li Z. et al., 2015).

Species	Observed peaks(cm^{-1})	Vibrational description
Methyl parathion (MP)	858.5	$\nu(\text{P-O})$
	1111.0	$\nu(\text{C-N})$
	1346.6	$\delta(\text{C-H})$
	1591.6	Phenyl stretching
Melamine (Me)	576.6	$\delta(\text{NCN})+\tau(\text{NH}_2)$
	687.4	Ring breathing
	978.6	$\delta(\text{CNC})+\tau(\text{NCN})$
	1496.5	$\delta(\text{NCN})+\omega(\text{NH}_2)$
	1549.9	$\nu(\text{CN})+\delta(\text{NH}_2)$
	1692.6	$\delta(\text{NH}_2)$

ω , wagging vibration; δ , bending vibration; ν , stretching vibration; τ , twisting vibration.

Sensitivity of SERS Sensor System Toward Targets

In order to determine the sensitivity of the SERS sensor, methyl parathion in ethanol and melamine in water were prepared at a range of concentrations from 1×10^{-4} M to 1×10^{-8} M. The strongest peaks at 1346.6 and 687.4 cm^{-1} were selected for concentration-dependence SERS studies of methyl parathion and melamine, respectively. **Figure 6A** depicted the Raman spectra of methyl parathion with concentrations varying from 1×10^{-4} M to 1×10^{-8} M. It was clear that the Raman intensities significantly decreased with decreased concentration of methyl parathion. Inset of **Figure 6A** represents the Raman spectra at low methyl parathion concentrations, showing a clearly distinguishable peak at 1346.6 cm^{-1} even at methyl parathion concentration of 10 nM. The result demonstrated that the wax/AuNPs-methyl parathion/AuNPs displays high sensitivity

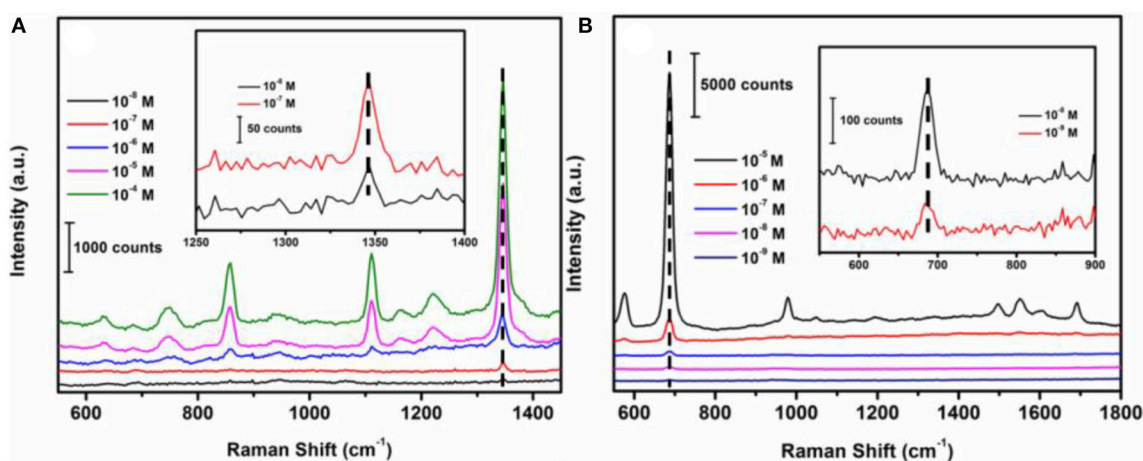
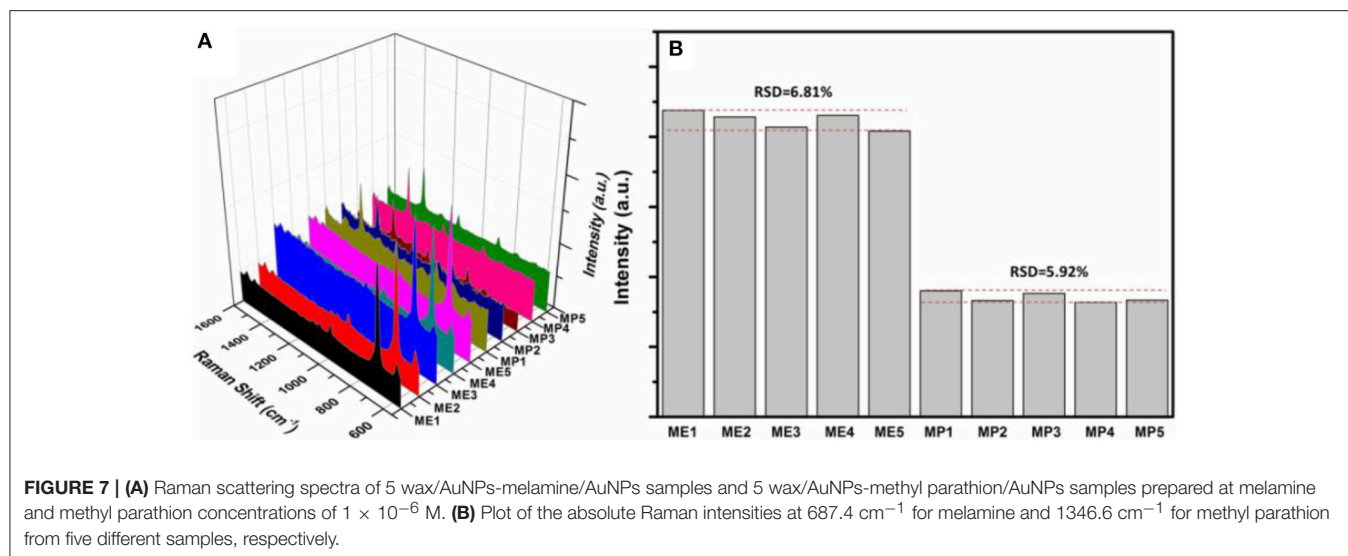


FIGURE 6 | Raman scattering spectra of wax/AuNPs-methyl parathion/AuNPs at different methyl parathion concentrations varied from 10^{-8} M to 10^{-4} M (A) and wax/AuNPs-melamine/AuNPs at different melamine concentrations varied from 10^{-9} M to 10^{-5} M (B).



with detection limit down to nanomolar level ($S/N > 3$) for methyl parathion. Similar results depicted in **Figure 6B** were obtained for melamine. Raman scattering spectra intensities obviously increased with increase of melamine concentrations. The Raman scattering spectra at low concentrations melamine were shown in inset of **Figure 6B**. A distinct peak at 687.4 cm^{-1} can be obtained at low melamine concentration of 1×10^{-9} M, which demonstrates that the wax/AuNPs-melamine/AuNPs can detect melamine at sub-nanomolar level ($S/N > 3$). These results proved that the wax/AuNPs-analyte/AuNPs based SERS strategy is highly sensitive toward both methyl parathion and melamine.

Reproducibility and Practicability

Excellent hydrophobicity of wax-coated surface favors the uniformity of the distribution of AuNPs-analyte/AuNPs on the substrate after drying, thus resulting in better reproducibility in SERS sensing. Also the use of a fiber-coupled portable Raman spectrometer is beneficial to the reproducibility, because the optical fiber collects signal from a much larger area, compared to the desktop Raman microscope where the laser beam is highly focused. As shown in **Figure 7A**, Raman scattering spectra of quintuplicate methyl parathion and melamine samples at an analyte concentration of 1×10^{-6} M were recorded. Similar peak intensities were obtained for both methyl parathion and melamine in all five samples. **Figure 7B** shows the absolute intensities for melamine and methyl parathion after subtraction of the background signal. As shown, the absolute intensities obtained were almost constant for methyl parathion and melamine, with a small relative standard deviation (RSD) of 6.81 and 5.92%, respectively, demonstrating a satisfactory reproducibility in SERS-based detection toward both analytes.

To study the feasibility of wax/AuNPs-analyte/AuNPs based SERS platform in real applications, lake water spiked with methyl parathion and milk spiked with melamine were prepared with desired analyte concentrations (1×10^{-5} M, 1×10^{-6} M, and 1×10^{-7} M). After sample

TABLE 2 | Recovery studies of methyl parathion in spiked lake water samples and melamine in spiked milks samples.

Spiked samples	Added amount (μM)	Recoveries (%)	RSD (%)
Lake water spiked with MP	10	98.6	9.03
	1	114.2	9.11
	0.1	97.3	6.58
Milk spiked with Me	10	68.6	11.09
	1	59.3	9.11
	0.1	66.4	5.27

processing as described in previous experimental section, the Raman spectra of the samples were collected. The Raman peak intensities at 1346.6 and 687.4 cm^{-1} were used to calculate the recovery for methyl parathion and melamine, respectively. As shown in **Table 2**, recoveries of methyl parathion in spiked lake water ranges from 97.3 to 114.2% with a relative standard deviation $< 9.11\%$, suggesting excellent recoveries for methyl parathion detection in lake water samples. However, low recoveries of melamine ranging from 59.3 to 68.6% were obtained in spiked milk samples. The low recoveries are likely caused by the sample treatment/melamine recovery procedure before Raman detection. In our study, to recover melamine in milk, the milk proteins and other macromolecules were denatured/precipitated using methanol, followed by centrifugation for removal. Denatured/precipitated proteins/macromolecules are naturally absorbents, and thus can adsorb small molecules like melamine, resulting in the loss of melamine in supernatant for the SERS detection. In spite of the relatively lower recovery, the maximum of melamine content of 2.5 ppm ($20 \mu\text{M}$) in milk regulated by many international agencies can be easily detected (Wu et al., 2012; Trapiella-Alfonso et al., 2013). These results have demonstrated that the wax/AuNPs-analyte/AuNPs based SERS sensing strategy holds great

potential in real applications for food safety and environment protection.

CONCLUSIONS

In summary, we have presented a versatile, rapid and low-cost SERS sensing platform enabled by AuNPs-analyte/AuNPs double-decker structure on wax-coated hydrophobic surface using a portable Raman spectrometer. The method has been successfully applied for sensitive and selective detection of methyl parathion and melamine. Wax coating provides a universal, simple and low-cost method to produce highly hydrophobic substrates, which can enhance the sensitivity and reproducibility of SERS detection of analytes in water or polar solvents. In addition, by coating another layer of AuNPs on AuNPs-analyte to form double-decker structure, the sensitivity of the method is further improved significantly due to the formation of more “hot spots.” Remarkable recovery for methyl parathion spiked into lake water and acceptable recovery for melamine spiked into milk have been obtained, indicating good applicability and feasibility of the developed sensor platform for real applications. All these features demonstrated that the wax/AuNPs-analyte/AuNPs

based SERS sensing strategy can potentially be used in sensing trace amount of chemicals for food and environmental safety applications.

AUTHOR CONTRIBUTIONS

HW conducted the SERS experiments and initiated the writing of the manuscript. YiL and JZ synthesized AuNPs. YH and QD discussed the results and processed data. CH and JZ revised the manuscript. DH and YuL designed the experiment, managed the project, and finalized the manuscript.

ACKNOWLEDGMENTS

This work was performed in part at the Biosciences Electron Microscopy Facility of the University of Connecticut. CH and DH appreciate the financial support from Chongqing Science and Technology Commission (CSTC2015shmszxl20097), the National Natural Science Foundation of China (NO. 31171684). YL and JZ thank the partial support from NSF. YH appreciates the support of GE fellowship. We also thank Prof. Anson Ma for his help in contact angle test.

REFERENCES

- Albrecht, M. G., and Creighton, J. A. (1977). ChemInform Abstract: ANOMALOUSLY INTENSE RAMAN SPECTRA OF PYRIDINE AT A SILVER ELECTRODE. *Cheminform* 8, 5215–5217. doi: 10.1002/chin.197901013
- Alsammarrha, F. K., and Lin, M. (2017). Using standing gold nanorod arrays as surface-enhanced Raman spectroscopy (SERS) substrates for detection of carbaryl residues in fruit juice and milk. *J. Agric. Food Chem.* 65, 666–674. doi: 10.1021/acs.jafc.6b04774
- Camden, J. P., Dieringer, J. A., Wang, Y., Masiello, D. J., Marks, L. D., Schatz, G. C., et al. (2008). Probing the structure of single-molecule surface-enhanced Raman scattering hot spots. *J. Am. Chem. Soc.* 130, 12616–12617. doi: 10.1021/ja8051427
- Cao, X., Hong, S., Jiang, Z., She, Y., Wang, S., Zhang, C., et al. (2017). SERS-active metal-organic frameworks with embedded gold nanoparticles. *Analyst* 142, 2640–2647. doi: 10.1039/C7AN00534B
- Cheung, M., Lee, W. W. Y., Mcracken, J. N., Larmour, I. A., Brennan, S., and Bell, S. E. J. (2016). Raman analysis of dilute aqueous samples by localized evaporation of submicroliter droplets on the tips of superhydrophobic copper wires. *Anal. Chem.* 88, 4541–4547. doi: 10.1021/acs.analchem.6b00563
- Fleischmann, M., Hendra, P. J., and Mcquillan, A. J. (1974). Raman spectra of pyridine adsorbed at a silver electrode. *Chem. Phys. Lett.* 26, 163–166. doi: 10.1016/0009-2614(74)85388-1
- Fortuni, B., Fujita, Y., Ricci, M., Inose, T., Aubert, R., Lu, G., et al. (2017). A novel method for *in situ* synthesis of SERS-active gold nanostars on polydimethylsiloxane film. *Chem. Commun.* 53, 5121–5124. doi: 10.1039/C7CC01776F
- Freeman, R. G., Grabar, K. C., Allison, K. J., Bright, R. M., Davis, J. A., Guthrie, A. P., et al. (1995). Self-assembled metal colloid monolayers: an approach to SERS substrates. *Science* 267, 1629–1632. doi: 10.1126/science.267.5204.1629
- Frens, G. (1973). Controlled nucleation for the regulation of the particle size in monodisperse gold suspensions. *Nature* 241, 20–22.
- Giovannozzi, A. M., Rolle, F., Sega, M., Abete, M. C., Marchis, D., and Rossi, A. M. (2014). Rapid and sensitive detection of melamine in milk with gold nanoparticles by Surface Enhanced Raman Scattering. *Food Chem.* 159, 250–256. doi: 10.1016/j.foodchem.2014.03.013
- Haiss, W., Thanh, N. T., Aveyard, J., and Fernig, D. G. (2007). Determination of size and concentration of gold nanoparticles from UV-Vis spectra. *Anal. Chem.* 79, 4215–4221. doi: 10.1021/ac0702084
- He, L., Shi, J., Sun, X., Lin, M., Yu, P., and Li, H. (2011). Gold coated zinc oxide nanonecklaces as a SERS substrate. *J. Nanosci. Nanotechnol.* 11, 3509–3515. doi: 10.1166/jnn.2011.3736
- Hogard, M. L., Lunte, C. E., and Lunte, S. M. (2017). Detection of reactive aldehyde biomarkers in biological samples using solid-phase extraction pre-concentration and liquid chromatography with fluorescence detection. *Anal. Methods* 9, 1848–1854. doi: 10.1039/C6AY03327J
- Hu, Y., Feng, S., Gao, F., Li-Chan, E. C. Y., Grant, E., and Lu, X. (2015). Detection of melamine in milk using molecularly imprinted polymers-surface enhanced Raman spectroscopy. *Food Chem.* 176, 123–129. doi: 10.1016/j.foodchem.2014.12.051
- Ilkhani, H., Hughes, T., Li, J., Zhong, C. J., and Hepel, M. (2016). Nanostructured SERS-electrochemical biosensors for testing of anticancer drug interactions with DNA. *Biosens. Bioelectron.* 80, 257–264. doi: 10.1016/j.bios.2016.01.068
- Jayram, N. D., Aishwarya, D., Sonia, S., Mangalaraj, D., Kumar, P. S., and Rao, G. M. (2016). Analysis on superhydrophobic silver decorated copper Oxide nanostructured thin films for SERS studies. *J. Colloid Interface Sci.* 477, 209–219. doi: 10.1016/j.jcis.2016.05.051
- Jeanmaire, D. L., and Duynes, R. P. V. (1977). Surface Raman spectroelectrochemistry: Part I. Heterocyclic, aromatic, and aliphatic amines adsorbed on the anodized silver electrode. *J. Electroanal. Chem. Interfac. Electrochem.* 84, 1–20.
- Jiang, C., Ma, X., Xue, M., and Lian, H.-Z. (2017). Application of thermoresponsive hydrogel/gold nanorods composites in the detection of diquat. *Talanta* 174, 192–197. doi: 10.1016/j.talanta.2017.06.010
- Kim, A., Barcelo, S. J., Williams, R. S., and Li, Z. (2012). Melamine sensing in milk products by using Surface Enhanced Raman Scattering. *Anal. Chem.* 84, 9303–9309. doi: 10.1021/ac302025q
- Kleinman, S. L., Frontiera, R. R., Henry, A.-I., Dieringer, J. A., and Van Duyne, R. P. (2013). Creating, characterizing, and controlling chemistry with SERS hot spots. *Phys. Chem. Chem. Phys.* 15, 21–36. doi: 10.1039/C2CP42598J
- Kubackova, J., Fabriciova, G., Miskovsky, P., Jancura, D., and Sanchez-Cortes, S. (2015). Sensitive Surface-Enhanced Raman Spectroscopy (SERS) detection of

- organochlorine pesticides by alkyl dithiol-functionalized metal nanoparticles-induced plasmonic hot spots. *Anal. Chem.* 87, 663–669. doi: 10.1021/ac503672f
- Kurzatowska, K., Santiago, T., and Hepel, M. (2017). Plasmonic nanocarrier grid-enhanced Raman sensor for studies of anticancer drug delivery. *Biosens. Bioelectron.* 91, 780–787. doi: 10.1016/j.bios.2017.01.049
- Lee, S., Choi, J., Chen, L., Park, B., Kyong, J. B., Seong, G. H., et al. (2007). Fast and sensitive trace analysis of malachite green using a surface-enhanced Raman microfluidic sensor. *Anal. Chim. Acta* 590, 139–144. doi: 10.1016/j.aca.2007.03.049
- Li, J., Chen, L., Lou, T., and Wang, Y. (2011). Highly sensitive SERS detection of As³⁺ ions in aqueous media using glutathione functionalized silver nanoparticles. *ACS Appl. Mater. Interfaces* 3:3936. doi: 10.1021/am200810x
- Li, J. J., An, H. Q., Zhu, J., and Zhao, J. W. (2015). Improve the Surface Enhanced Raman Scattering of gold nanorods decorated graphene oxide: the effect of CTAB on the electronic transition. *Appl. Surf. Sci.* 347, 856–860. doi: 10.1016/j.apsusc.2015.04.194
- Li, X., Lee, H. K., Phang, I. Y., Lee, C. K., and Ling, X. Y. (2014). Superhydrophobic-oleophobic Ag nanowire platform: an analyte-concentrating and quantitative aqueous and organic toxin surface-enhanced Raman scattering sensor. *Anal. Chem.* 86, 10437–10444. doi: 10.1021/ac502955w
- Li, Z., Meng, G., Huang, Q., Hu, X., He, X., Tang, H., et al. (2015). Ag nanoparticle-grafted PAN-nanohump array films with 3D high-density hot spots as flexible and reliable SERS substrates. *Small* 11, 5452–5459. doi: 10.1002/smll.201501505
- Lim, D. K., Jeon, K. S., Kim, H. M., Nam, J. M., and Suh, Y. D. (2010). Nanogap-engineerable Raman-active nanodumbbells for single-molecule detection. *Nat. Mater.* 9, 60–67. doi: 10.1038/nmat2596
- Liu, H. L., Cao, J., Hanif, S., Yuan, C., Pang, J., Levicky, R., et al. (2017). Size-Controllable Gold Nanopores with High SERS Activity. *Anal. Chem.* 89, 10407–10413. doi: 10.1021/acs.analchem.7b02410
- Lou, T., Wang, Y., Li, J., Peng, H., Xiong, H., and Chen, L. (2011). Rapid detection of melamine with 4-mercaptopyridine-modified gold nanoparticles by surface-enhanced Raman scattering. *Anal. Bioanal. Chem.* 401, 333–338. doi: 10.1007/s00216-011-5067-3
- Mircescu, N. E., Oltean, M., Chiş, V., and Leopold, N. (2012). FTIR, FT-Raman, SERS and DFT study on melamine. *Vib. Spectrosc.* 62, 165–171. doi: 10.1016/j.vibspec.2012.04.008
- Nguyen, T. H. D., Zhang, Z., Mustapha, A., Li, H., and Lin, M. (2014). Use of graphene and gold nanorods as substrates for the detection of pesticides by Surface Enhanced Raman Spectroscopy. *J. Agric. Food Chem.* 62, 10445–10451. doi: 10.1021/jf5036417
- Özyürek, M., Baki, S., Gungor, N., Celik, S. E., Guclu, K., and Apak, R. (2012). Determination of biothiols by a novel on-line HPLC-DTNB assay with post-column detection. *Anal. Chim. Acta* 750, 173–181. doi: 10.1016/j.aca.2012.03.056
- Peng, B., Li, G., Li, D., Dodson, S., Zhang, Q., Zhang, J., et al. (2013). Vertically aligned gold nanorod monolayer on arbitrary substrates: self-assembly and femtomolar detection of food contaminants. *ACS Nano* 7, 5993–6000. doi: 10.1021/nn401685p
- Rajapandiyani, P., Tang, W.-L., and Yang, J. (2015). Rapid detection of melamine in milk liquid and powder by surface-enhanced Raman scattering substrate array. *Food Control* 56, 155–160. doi: 10.1016/j.foodcont.2015.03.028
- Schwartzberg, A. M., Grant, C. D., Wolcott, A., Talley, C. E., Huser, T. R., Bogomolni, R., et al. (2004). Unique gold nanoparticle aggregates as a highly active Surface-Enhanced Raman Scattering Substrate. *J. Phys. Chem. B* 108, 19191–19197. doi: 10.1021/jp048430p
- Tan, M. J., Hong, Z.-Y., Chang, M.-H., Liu, C.-C., Cheng, H.-F., Loh, X. J., et al. (2017). Metal carbonyl-gold nanoparticle conjugates for highly sensitive SERS detection of organophosphorus pesticides. *Biosens. Bioelectron.* 96, 167–172. doi: 10.1016/j.bios.2017.05.005
- Tian, X. D., Liu, B. J., Li, J. F., Yang, Z. L., Ren, B., and Tian, Z. Q. (2013). SHINERS and plasmonic properties of Au Core SiO₂ shell nanoparticles with optimal core size and shell thickness. *J. Raman Spectrosc.* 4, 994–998. doi: 10.1002/jrs.4317
- Trapiella-Alfonso, L., Costa-Fernandez, J. M., Pereiro, R., and Sanz-Medel, A. (2013). Synthesis and characterization of haptent-quantum dots bioconjugates: application to development of a melamine fluorescent immunoassay. *Talanta* 106, 243–248. doi: 10.1016/j.talanta.2013.01.027
- Vesely, P., Lusk, L., Basarova, G., Seabrooks, J., and Ryder, D. (2003). Analysis of aldehydes in beer using solid-phase microextraction with on-fiber derivatization and gas chromatography/mass spectrometry. *J. Agric. Food Chem.* 51, 6941–6944. doi: 10.1021/jf034410t
- Wallace, R. A., Charlton, J. J., Kirchner, T. B., Lavrik, N. V., Datskos, P. G., and Sepaniak, M. J. (2014). Superhydrophobic analyte concentration utilizing colloid-pillar array SERS substrates. *Anal. Chem.* 86, 11819–11825. doi: 10.1021/ac5033947
- Wang, Y., Wang, H., Wang, Y., Shen, Y., Xu, S., and Xu, W. (2016). Plasmon-driven dynamic response of a hierarchically structural silver-decorated nanorod array for sub-10 nm nanogaps. *ACS Appl. Mater. Interfaces* 8, 15623–15629. doi: 10.1021/acsami.6b04173
- Wang, Y., Yan, B., and Chen, L. (2013). SERS tags: novel optical nanoprobe for bioanalysis. *Chem. Rev.* 113, 1391–1428. doi: 10.1021/cr300120g
- Wu, B., Wang, Z., Zhao, D., and Lu, X. (2012). A novel molecularly imprinted impedimetric sensor for melamine determination. *Talanta* 101, 374–381. doi: 10.1016/j.talanta.2012.09.044
- Yu, Z., Park, Y., Chen, L., Zhao, B., Jung, Y. M., and Cong, Q. (2015). Preparation of a superhydrophobic and peroxidase-like activity array chip for H₂O₂ sensing by Surface-Enhanced Raman Scattering. *ACS Appl. Mater. Interfaces* 7, 23472–23480. doi: 10.1021/acsami.5b08643
- Zhang, C., You, E., Jin, Q., Yuan, Y., Xu, M., Ding, S., et al. (2017). Observing the dynamic “hot spots” on two-dimensional Au nanoparticles monolayer film. *Chem. Commun.* 53, 6788–6791. doi: 10.1039/C7CC03020G
- Zhou, Q., Meng, G., Wu, N., Zhou, N., Chen, B., Li, F., et al. (2016). Dipping into a drink: Basil-seed supported silver nanoparticles as surface-enhanced Raman scattering substrates for toxic molecule detection. *Sensors Actuat. B Chem.* 223, 447–452. doi: 10.1016/j.snb.2015.09.115

Conflict of Interest Statement: The authors declare that the research was conducted in the absence of any commercial or financial relationships that could be construed as a potential conflict of interest.

Copyright © 2018 Wu, Luo, Huang, Dong, Hou, Huo, Zhao and Lei. This is an open-access article distributed under the terms of the Creative Commons Attribution License (CC BY). The use, distribution or reproduction in other forums is permitted, provided the original author(s) and the copyright owner(s) are credited and that the original publication in this journal is cited, in accordance with accepted academic practice. No use, distribution or reproduction is permitted which does not comply with these terms.